2.4 NONCLINICAL OVERVIEW

TABLE OF CONTENTS

LIST OF ABBREVIATIONS AND DEFINITION OF TERMS

A:G	Albumin:globulin ratio
ACE	Angiotension-converting enzyme
ADME	Absorption, distribution, metabolism, excretion
ALC-0159	Proprietary PEG-lipid included as an excipient in the LNP formulation used in BNT162b2
ALC-0315	Proprietary amino-lipid included as an excipient in the LNP formulation used in BNT162b2
ALT	Alanine aminotransferase
AST	Aspartate aminotransferase
BAL	Bronchoalveolar lavage
CAS	Chemical abstracts service
CBER	Center for Biologics Evaluation and Research
CD	Cluster of differentiation
COVID-19	Coronavirus Disease 2019
DART	Developmental and reproductive toxicity
DNA	Deoxyribonucleic acid
DSPC	1,2-distearoyl-sn-glycero-3-phosphocholine
ELISA	Enzyme-linked immunosorbent assay
EUA	Emergency Use Authorization
F0	Parental generation administered vaccine
F1	First generation offspring of F0 generation
GD	Gestation day
GGT	Gamma-glutamyl transferase
GLP	Good Laboratory Practice
H	Human (in metabolite scheme)
[^{3}H]-CHE	Radiolabeled [Cholesteryl-1,2-^{3}H(N)]-Cholesteryl Hexadecyl Ether
HGB	Hemoglobin
IFN	Interferon
IgG	Immunoglobulin G
IL	Interleukin
IM	Intramuscular(ly)
IND	Investigational New Drug Application
IV	Intravenous(ly)
LC/MS	Liquid chromatography-tandem mass spectrometry
LD	Lactation day
LNP	Lipid-nanoparticle
Luc	Luciferase (from firefly *Pyractomena lucifera*)
LUC	Large unstained cell
Mk	Monkey (in metabolite scheme)
Mo	Mouse (in metabolite scheme)
modRNA	Nucleoside-modified mRNA
mRNA	Messenger RNA
NA	Not applicable

LIST OF ABBREVIATIONS AND DEFINITION OF TERMS - CONTINUED

NHP	Nonhuman primate
OECD	Organisation for Economic Co-operation and Development
P2 S	Spike protein P2 mutant
PEG	Polyethylene glycol
PK	Pharmacokinetics
PLT	Platelet
PND	Postnatal day
PT	Prothrombin time
QC	Quality control review
QW	Once weekly
R	Rat (in metabolite scheme)
RBC	Red blood cell
RBD	Receptor binding domain
RdRp	RNA-dependent RNA-polymerase
RDW	Red cell distribution width
RETIC	Reticulocyte
RNA	Ribonucleic acid
RT-PCR	Reverse transcription-polymerase chain reaction
S	SARS-CoV-2 spike glycoprotein
S1	S1 domain of the SARS-CoV-2 spike glycoprotein
S9	Supernatant fraction obtained from liver homogenate by centrifuging at 9000 g
SARS	Severe Acute Respiratory Syndrome
SARS-CoV-2	Severe acute respiratory syndrome coronavirus 2; coronavirus causing COVID-19
Tfh	T follicular helper cell
Th1	Type 1 T helper cells
TK	Toxicokinetic
TNF	Tumor necrosis factor
V8	Variant 8; P2 S
V9	Variant 9; P2 S
WBC	White blood cell
WHO	World Health Organization

2.4.1. OVERVIEW OF NONCLINICAL TESTING STRATEGY

BNT162b2 (BioNTech code number BNT162, Pfizer code number PF-07302048) is an investigational vaccine intended to prevent COVID-19, which is caused by SARS-CoV-2. BNT162b2 is a nucleoside modified mRNA (modRNA) expressing full-length S with two proline mutations (P2) to lock the transmembrane protein in an antigenically optimal prefusion conformation (Pallesen et al, 2017; Wrapp et al, 2020). The vaccine is formulated in lipid nanoparticles (LNPs). The LNP is composed of 4 lipids: ALC-0315, ALC-0159, DSPC, and cholesterol. Other excipients in the formulation include sucrose, NaCl, KCl, Na_2HPO_4, and KH_2PO_4. The dose selected for BNT162b2, with efficacy demonstrated in Phase 2/3 clinical evaluation and intended for commercial use, is 30 µg administered IM as two doses given 21 days apart.

In nonclinical studies, two variants of BNT162b2 were tested; designated "variant 8" and "variant 9" (V8 and V9, respectively). The variants differ only in their codon optimization sequences which are designed to improve antigen expression, otherwise the amino acid sequences of the encoded antigens are identical. Only BNT162b2 (V9) has been evaluated in the clinic, is currently authorized under EUA, and is the subject of this BLA application. The characteristics of each variant are described in the table below (Table 2.4.1-1).

Table 2.4.1-1. Nomenclature of the Vaccine Candidates

Product Code	RNA Platform	Antigen Variant	Description/Translated Protein	Variant Code	GLP Tox Data	Clinical Candidate
BNT162b2	modRNA	V8[a]	P2 S	RBP020.1	Yes	No
BNT162b2	**modRNA**	**V9[a]**	**P2 S**	**RBP020.2**	**Yes**	**Yes**

a. The V8 and V9 variants of the P2 S antigen have the same amino acid sequence. Different codon optimizations were used for their ribonucleotide sequences.

Bold: BNT162b2 (V9) vaccine candidate submitted for licensure.

The primary pharmacology, distribution, metabolism, and safety of BNT162b2 were evaluated in nonclinical pharmacology, pharmacokinetic, and toxicity studies in vitro and in vivo (Table 2.4.1-2).

Immunogenicity of BNT162b2 was evaluated in mice (2.4.2.1.3), rats (2.4.2.1.5) and nonhuman primates (2.4.2.1.4). For assessment of serum antibody responses in mice and rats, S1 and RBD-binding IgG responses were tested by an ELISA. Functional antibody responses were tested by a SARS-CoV-2 pseudotype neutralization assay (pVNT). In nonhuman primate studies, S1-binding IgG responses were tested in a direct Luminex-based immunoassay (dLIA) and functional antibody responses were assessed in a SARS-CoV-2 neutralization assay. S-specific T cell responses were assessed in mouse and nonhuman primate studies in an IFNγ ELISpot and by intracellular cytokine staining flow cytometry-based analysis of the Th1/Th2 profile using splenocytes.

A SARS-CoV-2 challenge study in BNT162b2 (V9)-immunized nonhuman primates was also conducted to assess protection against infection and to demonstrate lack of disease enhancement (Section 2.4.2.1.4.2).

Platform properties that support BNT162b2 were initially demonstrated with non-SARS-CoV-2 antigens. Non-GLP in vivo testing of an LNP-formulated modRNA encoding luciferase examined biodistribution in BALB/c mice and Wistar Han rats after IM injection (Section 2.4.3.4) and the PK of the two novel excipients in the LNP formulation, ALC-0315 and ALC-0159, in Wistar Han rats (Section 2.4.3.3). In addition, the metabolism of ALC-0315 and ALC-0159 was evaluated in mouse, rat, monkey, and human blood, liver microsomes, S9 fractions, and hepatocytes and in vivo in rat plasma, urine, feces, and liver samples from the PK study (Table 2.4.1-2; Section 2.4.3.5).

BNT162b2 (V8) and (V9) have been studied in GLP-compliant repeat-dose toxicity studies in rats (Table 2.4.1-2). Two GLP repeat-dose toxicity studies for BNT162b2 (V8) and BNT162b2 (V9), one study for each variant, have been completed. The study designs are described in Section 2.4.4 and are based on WHO guidelines for vaccine development (WHO, 2005). A DART study with BNT162b2 (V9) in rats has also been completed. No additional toxicity studies are planned for BNT162b2.

IM administration was chosen for the toxicity studies as this is the intended route of administration. Rats were chosen for toxicity assessments as they are a commonly used animal species for the evaluation of toxicity, and they mount an antigen-specific immune response to vaccination with BNT162b2.

The design of the nonclinical repeat-dose toxicity studies was consistent with the WHO Guidelines on Nonclinical Evaluation of Vaccines, the EMA Note for Guidance on Preclinical Pharmacological and Toxicological Testing of Vaccines, and Japan guidance on the nonclinical safety assessment of vaccines. In addition, the 2020 CBER guidance on "Development and Licensure of Vaccines to Prevent COVID-19" (US FDA, 2020) was considered when assembling the nonclinical safety licensure package as well as feedback from regulatory agencies. All GLP-compliant studies were conducted in accordance with Good Laboratory Practice for Nonclinical Laboratory Studies, Code of US Federal Regulations (21 CFR Part 58), in an OECD Mutual Acceptance of Data member state. All nonclinical studies described herein were conducted by or for Pfizer Inc or BioNTech RNA Pharmaceuticals GmbH. The location of records for inspection is included in each final study report.

Table 2.4.1-2. Nonclinical Studies

Study Number	Study Type	Species / Test System	Test Item	Dose [RNA]	Cross reference
Pharmacology - BNT162b2 studies					
R-20-0085	In vivo immunogenicity	BALB/c mice	BNT162b2 (V9)	0.2, 1, 5 µg	Section 2.4.2.1.3
R-20-0112	In vivo immunogenicity	BALB/c mice	BNT162a1, BNT162b1, BNT162b2 (V9), BNT162c2	5 µg	Section 2.4.2.1.3
R-20-0211	In vitro protein expression	Cell culture	BNT162b2 (V9)	varied	Section 2.4.2.1.2
VR-VTR-10741	In vitro protein expression	Cell culture	BNT162b2 (V9)	varied	Section 2.4.2.1.2
VR-VTR-10671	In vivo immunogenicity and SARS-CoV-2 challenge	Rhesus macaques	BNT162b2 (V9)	30 and 100 µg	Section 2.4.2.1.4
ADME					
PF-07302048 _06Jul20_072424	PK of ALC-0315 and ALC-0159	Wistar Han Rats	modRNA encoding luciferase formulated in LNP comparable to BNT162b2	1 mg/kg	Section 2.4.3.3
R-20-0072	In vivo distribution	BALB/c mice	modRNA encoding luciferase formulated in LNP comparable to BNT162b2	2 µg	Section 2.4.3.4
185350	In vivo distribution	Wistar Han Rats	modRNA encoding luciferase formulated in LNP comparable to BNT162b2 with trace amounts of [^{3}H]-CHE as non-diffusible label	50 µg	Section 2.4.3.4
01049-20008	In vitro metabolism	CD-1/ICR mouse, Wistar Han and/or Sprague Dawley rat, cynomolgus monkey and human liver microsomes, S9 fraction, hepatocytes	ALC-0315	NA	Section 2.4.3.5
01049-20009					
01049-20010					
01049-20020			ALC-0159	NA	
01049-20021					
01049-20022					

Table 2.4.1-2. Nonclinical Studies - Continued

Study Number	Study Type	Species / Test System	Test Item	Dose [RNA]	Cross reference
PF-07302048 _05Aug20_043725	In vitro and in vivo metabolism	Blood, liver S9 fractions and hepatocytes from CD-1 mouse, Wistar Han rat, cynomolgus monkey and human. In vivo samples from Wistar Han rat plasma, urine, feces, and liver	In vitro: ALC-0315 and ALC-0159 In vivo: modRNA encoding luciferase formulated in LNP comparable to BNT162b2	1 mg/kg modRNA (in vivo samples)	Section 2.4.3.5
Toxicology – Studies with BNT162b2 variants					
38166	Repeat-dose toxicity	Wistar Han Rats	BNT162b2 (V8)	100 µg	Section 2.4.4.3
20GR142	Repeat-dose toxicity	Wistar Han Rats	BNT162b2 (V9)	30 µg	Section 2.4.4.3
20256434	Development and Reproductive Toxicity	Wistar Han Rats	BNT162b2 (V9)	30 µg	Section 2.4.4.6

2.4.2. PHARMACOLOGY

2.4.2.1. Primary Pharmacodynamics

2.4.2.1.1. Summary

BNT162b2 (BioNTech code number BNT162, Pfizer code number PF-07302048) is a nucleoside-modified mRNA (modRNA) vaccine that encodes the SARS-CoV-2 full-length spike glycoprotein (S). The glycoprotein encoded by both BNT162b2 variants includes two amino acid substitutions to proline (P2 S) locking the transmembrane protein in an antigenically optimal prefusion conformation (Wrapp et al, 2020; Pallesen et al, 2017). The RNA is formulated with functional and structural lipids, which protect the RNA from degradation and enable transfection of the RNA into host cells after IM injection. S is a major target of virus neutralizing antibodies and is a key antigen for vaccine development. The well-resolved trimeric prefusion structure and the high affinity binding to ACE2 and human neutralizing antibodies demonstrate that the recombinant P2 S authentically presents the ACE2 binding site and other epitopes targeted by many SARS-CoV-2 neutralizing antibodies.

In vitro studies and in vivo studies in mice and nonhuman primates demonstrate the mechanism of action for this RNA-based vaccine, which is to encode SARS-CoV-2 S that induces an immune response characterized by both a strong neutralizing antibody response and Th1-type $CD4^+$ and an $IFN\gamma^+$ $CD8^+$ T-cell response. BNT162b2 immunization protected rhesus macaques from infectious SARS-CoV-2 challenge, with reduced detection of viral RNA in vaccine-immunized animals compared to saline-immunized animals and with no evidence of clinical exacerbation.

2.4.2.1.2. BNT162b2, A Lipid Nanoparticle Encapsulated RNA Vaccine Encoding the SARS-CoV-2 P2 S as a Vaccine Antigen

BNT162b2 is based on a nucleoside-modified mRNA (modRNA) platform technology. Vaccination with modRNA formulated in LNPs is characterized by strong expansion of Th1-skewed antigen-specific T follicular helper (Tfh) cells, which stimulate and expand germinal center B cells, thereby resulting in particularly strong, long lived, high-affinity antibody responses (Sahin et al, 2014; Pardi et al, 2018). ModRNA vaccine candidates against other infectious diseases induce strong antibody responses and prime and expand multifunctional $CD4^+$ and $CD8^+$ T cells (Pardi et al, 2017; Pardi et al, 2018).

SARS-CoV-2 S is a large, trimeric glycoprotein that exists predominantly in a prefusion conformation on the virion (Ke et al, 2020). It is cleaved by furin into an N-terminal S1 and a C-terminal S2 fragment. S attaches to the host cell receptor, ACE2, by its receptor binding domain which is contained in the S1 furin cleavage fragment. Spontaneously and during cell entry, the S1 fragment dissociates, and the S2 fragment undergoes a fold-back rearrangement to the post-fusion conformation in a process that facilitates fusion of viral and host cell membranes. S is the main target of virus neutralizing antibodies (Zakhartchouk et al, 2007; Yong et al, 2019). Most of the antibodies with SARS-CoV-2 neutralizing activity are directed against the RBD (Jiang et al, 2020; Zost et al, 2020).

Figure 2.4.2-1. Schematic of the Organization of the SARS-CoV-2 S Glycoprotein

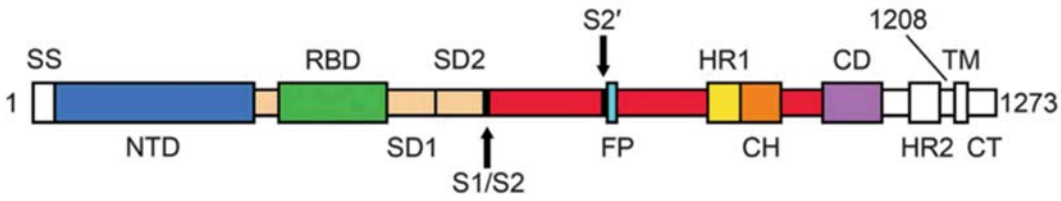

The S1 furin cleavage fragment includes the signal sequence (SS), the N terminal domain (NTD), the receptor binding domain (RBD, which binds the human cellular receptor, ACE-2), subdomain 1 (SD1), and subdomain 2 (SD2). The furin cleavage site (S1/S2) separates S1 from the S2 fragment, which contains the S2 protease cleavage site (S2′) followed by a fusion peptide (FP), heptad repeats (HR1 and HR2), a central helix (CH) domain, the connector domain (CD), the transmembrane domain (TM) and a cytoplasmic tail (CT).
Source: modified from Wrapp et al, 2020.

BNT162b2 (V9) encodes a full-length P2 S transmembrane protein that contains two consecutive prolines introduced at amino acid positions 986 and 987, between the central helix (CH) and heptad repeat 1 (HR1) (Figure 2.4.2-1) (Wrapp et al, 2020; Pallesen et al, 2017). Two codon optimized forms of the coding sequence for this antigen were tested preclinically and were designated “variant 8” and “variant 9” (V8 and V9), with the vaccine candidate tested clinically and being proposed for licensure or authorization, V9, expressed from a codon optimized RNA gene with a higher content of cytosine ribonucleotides for increased protein expression. The RNA-expressed P2 S is membrane bound and elicits a potent humoral neutralizing antibody response and Th1-type $CD4^+$ and $CD8^+$ cellular response to block virus infection and kill virus infected cells, respectively.

Efficient in vitro expression of the P2 S protein was demonstrated following in vitro transfection of cells with BNT162b2 RNA drug substance and BNT162b2 drug product. Electron cryomicroscopy analysis of purified recombinant P2 S, expressed from DNA encoding the same S amino acid sequence as BNT162b2 RNA (except for the addition of a C-terminal tag for protein purification) revealed high similarity to previously reported structures (Cai et al, 2020). The well-resolved trimeric prefusion structure and the high affinity binding to ACE2 and human neutralizing antibodies demonstrate that the recombinant full-length P2 S protein authentically presents the ACE-2 binding site.

2.4.2.1.3. Immunogenicity of BNT162b2 (V9) in Mice

BNT162b2 was highly immunogenic in mice with strong antigen-binding IgG and high titer neutralizing antibody responses together with a Th1-phenotype $CD4^+$ response as well as an $IFN\gamma^+$, $IL\text{-}2^+$ $CD8^+$ T-cell response after a single immunization. Total IgG ELISA showed that the vaccine induced a strong, dose-dependent IgG response that recognizes S1 and the RBD and elicited high neutralizing titers in a pseudotype neutralization assay.

Stimulation of fresh splenocytes, collected 28 days after immunization, with an S protein specific overlapping peptide pool demonstrated robust $CD4^+$ and $CD8^+$ T-cell IFNγ responses and a Th1-dominant profile was demonstrated in quantification of cytokines (IL-2 and IFNγ) in the corresponding culture supernatants.

In summary, BNT162b2 induced a strong, neutralizing antibody response. $CD4^+$ and $CD8^+$ T-cell responses were detectable 12 and 28 days after one immunization and exhibited a Th1-dominant T cell response characteristic of RNA-based vaccines.

2.4.2.1.4. Evaluation of BNT162b2 (V9) Immunogenicity and Protection Against SARS-CoV-2 Challenge in Rhesus Macaques

BNT162b2 was assessed for immunogenicity and for protection against an infectious SARS-CoV-2 challenge in rhesus macaques. SARS-CoV-2 infection in humans manifests as both asymptomatic infection and as the disease COVID-19, with diverse signs, symptoms, and levels of severity. Based on published reports, SARS-CoV-2 challenged rhesus macaques develop an acute, transient infection in the upper and lower respiratory tract and have evidence of viral replication in the gastrointestinal tract, similar to humans (Zou et al, 2020; Kim et al, 2020). Varying degrees of pulmonary inflammation, primarily at the peak of infection at approximately Day 2 to 4 post-challenge, have been reported in the literature (Munster et al, 2020). The human and rhesus ACE-2 receptor have 100% amino acid identity at the critical binding residues, which may account for the fidelity of this SARS-CoV-2 animal model (Zhou et al, 2020).

2.4.2.1.4.1. Immunogenicity in Rhesus Macaques

Rhesus macaques immunized IM with 30 µg or 100 µg of BNT162b2 on Days 0 and 21 had readily detectable S1-binding IgG and SARS-CoV-2 neutralizing titers (NT50) as early as 14 days after a single immunization, with substantial increases following the second immunization. On Day 28, seven days after Dose 2 at the 30 µg dose level, the neutralizing geometric mean titer (GMT) reached 8-fold the GMT of a 38 member panel of human convalescent sera (HCS); at the 100 µg dose level, the neutralizing GMT was 18-fold the HCS GMT. The HCS sera were drawn from SARS-CoV-2 infected individuals 18 to 83 years of age, at least 14 days after PCR-confirmed diagnosis and at a time when individuals were asymptomatic. The HCS panel provides a currently accessible benchmark to judge the quality of the humoral immune response to the vaccine. A decline of both, S1-binding IgG levels and neutralizing titers, was observed out to the latest measured time point (Day 56) but remained above the neutralizing GMT and the S1-binding geometric mean concentration (GMC) of the HCS.

As seen following mouse immunization, strong S-specific Th1-dominant $IFN\gamma^+$ T-cell responses were detected in all immunized rhesus macaques. By intracellular cytokine staining analysis, there was a dose-dependent increase in S-specific $CD4^+$ T cell responses with a strong Th1-bias evidenced by high frequency of $IFN\gamma^+$, $IL\text{-}2^+$, or $TNF\text{-}\alpha^+$ cells. Notably, $CD8^+$ T-cell responses were also detectable in BNT162b2-immunized animals.

2.4.2.1.4.2. SARS-CoV-2 Challenge of BNT162b2 (V9)-Immunized Nonhuman Primates

Groups of 2-4 year old male rhesus macaques that had received two IM immunizations with 100 µg BNT162b2 V9 (n=6) or saline (Control; n=3) 21 days apart were challenged 55 days after the second immunization with 1.05×10^6 plaque forming units of SARS-CoV-2 (strain USA-WA1/2020), split equally between the intranasal (IN) and intratracheal (IT) routes, as

previously described (Singh et al, 2020) (VR-VTR-10671). SARS-CoV-2 RNA was measured by reverse transcription- quantitative polymerase chain reaction (RT-qPCR) in bronchoalveolar lavage fluid, nasal swabs, and oropharyngeal swabs. The difference in viral RNA detection in BAL fluid between BNT162b2-immunised and control-immunised rhesus macaques after challenge is highly statistically significant (by a nonparametric test, p=0.0014). None of the challenged animals showed clinical signs of significant illness, indicating that the 2-4 years old male rhesus challenge model is primarily an infection model for SARS-CoV-2, not a COVID-19 disease model. No radiographic or histological evidence of vaccine-elicited enhanced disease was observed. In summary, BNT162b2 provided complete protection from the presence of detectable viral RNA in the lungs compared to the saline control with no evidence of vaccine-elicited disease enhancement.

2.4.2.1.5. Immunogenicity Testing After Weekly Immunization of Rats in GLP Compliant Repeat Dose Toxicology Studies and a Developmental and Reproductive Toxicity Study

The nonclinical safety data package consists of two GLP-compliant repeat-dose rat toxicity studies, in which both BNT162b2 variants (V8 and V9) were evaluated, and a DART study, in which BNT162b2 (V9) was evaluated (Section 2.4.4). In all studies, Study 38166 (evaluating V8) as well as Study 20GR142 and Study 20256434 (evaluating V9), the vaccine candidates were immunogenic.

In Study 38166, male and female rats received three weekly IM doses of BNT162b2 (V8). Serum samples were collected from main study animals on Day 17 (two days after the third dose) at the end of the dosing phase and on Day 38 at the end of a 3-week recovery phase. The sera were analyzed by ELISA for IgG that bound S1 and RBD as well as for SARS-CoV-2-S pseudovirus neutralizing antibodies. The vaccine candidates elicited IgG that recognized S1 and RBD. After immunization, animals developed high titers of antigen-specific antibodies as well as pseudovirus neutralization titers.

In Study 20GR142, male and female rats received three weekly IM doses of BNT162b2 (V9). Serum samples were collected from study animals prior to vaccine administration, at the end of the dosing phase on Day 17 (two days after the third dose), and at the end of the 3-week recovery phase on Recovery Phase Day 21. Sera were analyzed for SARS-CoV-2 neutralizing antibodies. After immunization, BNT162b2 (V9) elicited SARS-CoV-2 neutralizing antibody responses in males and females at the end of the dosing and recovery phases of the study. SARS-CoV-2 neutralizing antibody responses were not observed in animals prior to vaccine administration or in saline-administered control animals.

In Study 20256434, female rats were administered 4 total IM doses of BNT162b2 (V9) 21 and 14 days prior to mating and on GD9 and GD20. Serum samples were collected from females prior to vaccine administration, just prior to mating (M0), at the end of gestation (GD21), and at the end of lactation (LD21) and offspring (fetuses on GD21 and pups on PND21). Sera were analyzed for SARS-CoV-2 neutralizing antibodies. After immunization, SARS-CoV-2 neutralizing titers were detected in all maternal females as well as in their offspring (fetuses and pups). SARS-CoV-2 neutralizing antibody titers were not observed in animals prior to vaccine administration or in saline-administered control animals.

2.4.2.2. Secondary Pharmacodynamics

No secondary pharmacodynamics studies were conducted with BNT162b2.

2.4.2.3. Safety Pharmacology

No safety pharmacology studies were conducted with BNT162b2 as they are not considered necessary for the development of vaccines according to the WHO guideline (WHO, 2005).

2.4.2.4. Pharmacodynamic Drug Interactions

Nonclinical studies evaluating pharmacodynamic drug interactions with BNT162b2 were not conducted as they are generally not considered necessary to support development and licensure of vaccine products for infectious diseases (WHO, 2005).

2.4.3. PHARMACOKINETICS

2.4.3.1. Brief Summary

Assessment of the ADME profile of BNT162b2 (BioNTech code number BNT162, Pfizer code number PF-07302048) included evaluating the PK and metabolism of two novel lipid excipients (ALC-0315 and ALC-0159) in the LNP and potential biodistribution of BNT162b2 using luciferase expression as a surrogate reporter. The luciferase reporter was used as it was a readily available reporter that has been widely used to develop an understanding of protein/organ expression (Chen et al, 2020; Elia et al, 2020; Fukuchi et al, 2020; Hassett et al, 2019; Truong et al, 2019; Barry et al, 2012; Jeon et al, 2006). An intravenous rat PK study, using LNPs with the identical lipid composition as BNT162b2, demonstrated that ALC-0315 and ALC-0159 distribute from the plasma to the liver. While there was no detectable excretion of either lipid in the urine, the percent of dose excreted unchanged in feces was ~1% for ALC-0315 and ~50% for ALC-0159.

The biodistribution of BNT162b2 was evaluated using luciferase expression as a surrogate reporter in BALB/c mice. Mice were administered a luciferase expressing modRNA formulated like BNT162b2, with the identical lipid composition. Luciferase expression was measured in vivo following luciferin application. Luciferase expression was identified at the injection site at 6 hours after injection and was not detected after 9 days. Expression in the liver was also present to a lesser extent at 6 hours after injection and was not detected by 48 hours after injection. The distribution was also examined in male and female Wistar Han rats using LNPs with a comparable lipid composition to BNT162b2 but with a surrogate luciferase RNA and containing trace amounts of radiolabeled [^{3}H]-CHE, a non-exchangeable, non-metabolizable lipid marker. The greatest mean concentration of LNP was found remaining in the injection site in both sexes. Total recovery (% of injected dose) of LNP outside the injection site was greatest in the liver and was much less in the spleen, adrenal glands, and ovaries.

The in vitro metabolism of ALC-0315 and ALC-0159 was evaluated in blood, liver microsomes, S9 fractions, and hepatocytes from mice, rats, monkeys, and humans. The in vivo metabolism was examined in rat plasma, urine, feces, and liver samples from the PK study. Metabolism of ALC-0315 and ALC-0159 appears to occur slowly in vitro and in vivo. ALC-0315 and ALC-0159 are metabolized by hydrolytic metabolism of the ester and amide functionalities, respectively, and this hydrolytic metabolism is observed across the species evaluated.

In summary, the nonclinical ADME studies indicate that the LNP distributes to the liver. Approximately 50% of ALC-0159 is excreted unchanged in feces, while metabolism played a role in the elimination of ALC-0315.

2.4.3.2. Methods of Analysis

No methods of analysis have been validated to support GLP TK studies of components of BNT162b2; however, a qualified LC/MS method was developed to support quantitation of the two novel LNP excipients for the non-GLP IV PK study in rats

(Study PF-07302048_06Jul20_072424). Methods for immunogenicity and efficacy studies are described in Section 2.6.2.12.

2.4.3.3. Absorption

2.4.3.3.1. In Vitro Absorption

No absorption studies were conducted for BNT162b2, as the administration route is IM.

2.4.3.3.2. Single-Dose Pharmacokinetics

An intravenous rat PK study (PF-07302048_06Jul20_072424; Tabulated Summary 2.6.5.3) was performed using LNPs containing surrogate luciferase RNA, with the identical lipid composition as BNT162b2. This study was conducted to explore the disposition of ALC-0315 and ALC-0159 that had reached the systemic circulation following IM administration; thus, the IV route was felt to be appropriate. The findings are depicted in Table 2.4.3-1 and Figure 2.4.3-1.

Table 2.4.3-1. PK of ALC-0315 and ALC-0159 in Wistar Han Rats After IV Administration of LNPs Containing Surrogate Luciferase RNA at 1 mg/kg

Analyte	Dose of Analyte (mg/kg)	Gender /N	t½ (h)	AUC_{inf} (µg•h/mL)	AUC_{last} (µg•h/mL)	Estimated fraction of dose distributed to liver (%)[a]
ALC-0315	15.3	Male/3[b]	139	1030	1020	60
ALC-0159	1.96	Male/3[b]	72.7	99.2	98.6	20

a. Calculated as highest mean amount in the liver (µg)/total mean dose (µg) of ALC-0315 or ALC-0159.
b. 3 animals per timepoint; non-serial sampling.

Figure 2.4.3-1. Plasma and Liver Concentrations of ALC-0315 and ALC-0159 in Wistar Han Rats After IV Administration of LNPs Containing Surrogate Luciferase RNA at 1 mg/kg

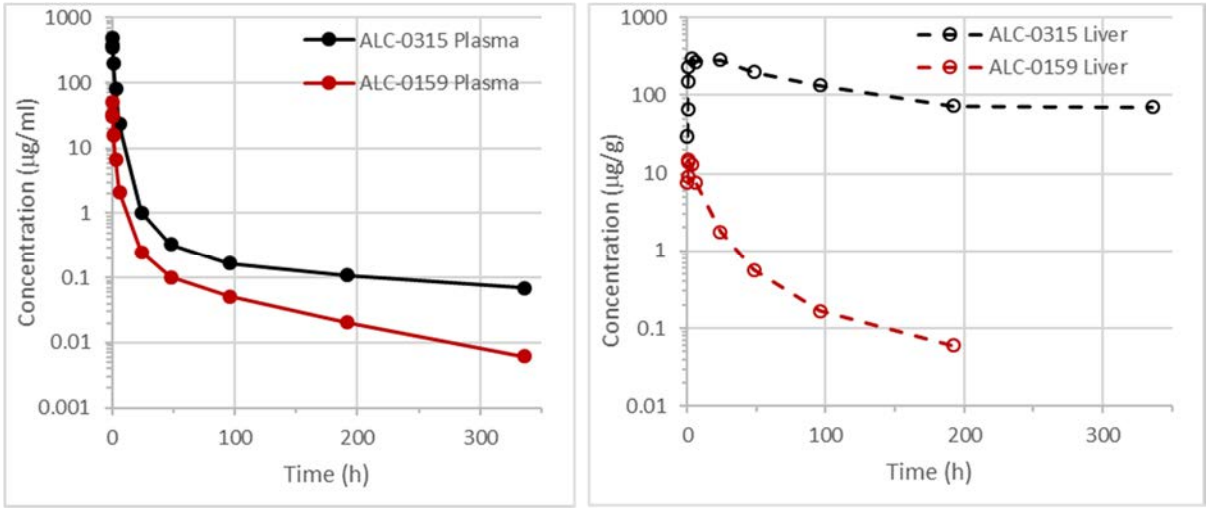

Pharmacokinetic studies have not been conducted with BNT162b2 and are generally not considered necessary to support the development and licensure of vaccine products for infectious diseases (WHO, 2005; WHO, 2014).

2.4.3.4. Distribution

In an in vivo study (R-20-0072; Tabulated Summary 2.6.5.5A), biodistribution was assessed using luciferase as a surrogate marker protein, with RNA encoding luciferase formulated like BNT162b2, with the identical lipid composition. The LNP-formulated luciferase-encoding modRNA was administered to BALB/c mice by IM injection of 1 µg each in the right and left hind leg (for a total of 2 µg). Using in vivo bioluminescence after injection of luciferin substrate, luciferase protein expression was detected at different timepoints at the site of injection and to a lesser extent, and more transiently, in the liver (Figure 2.4.3-2. Distribution to the liver is likely mediated by LNPs entering the blood stream. The luciferase expression at the injection sites dropped to background levels after 9 days. The repeat-dose toxicity study in rats showed no evidence of liver injury (Section 2.4.4.3).

The biodistribution of the antigen encoded by the RNA component of BNT162b2 is expected to be dependent on the LNP distribution and the results presented should be representative for the vaccine RNA platform, as the LNP-formulated luciferase-encoding modRNA had the same lipid composition.

Figure 2.4.3-2. Bioluminescence Emission in BALB/c Mice after IM Injection of an LNP Formulation of modRNA Encoding Luciferase

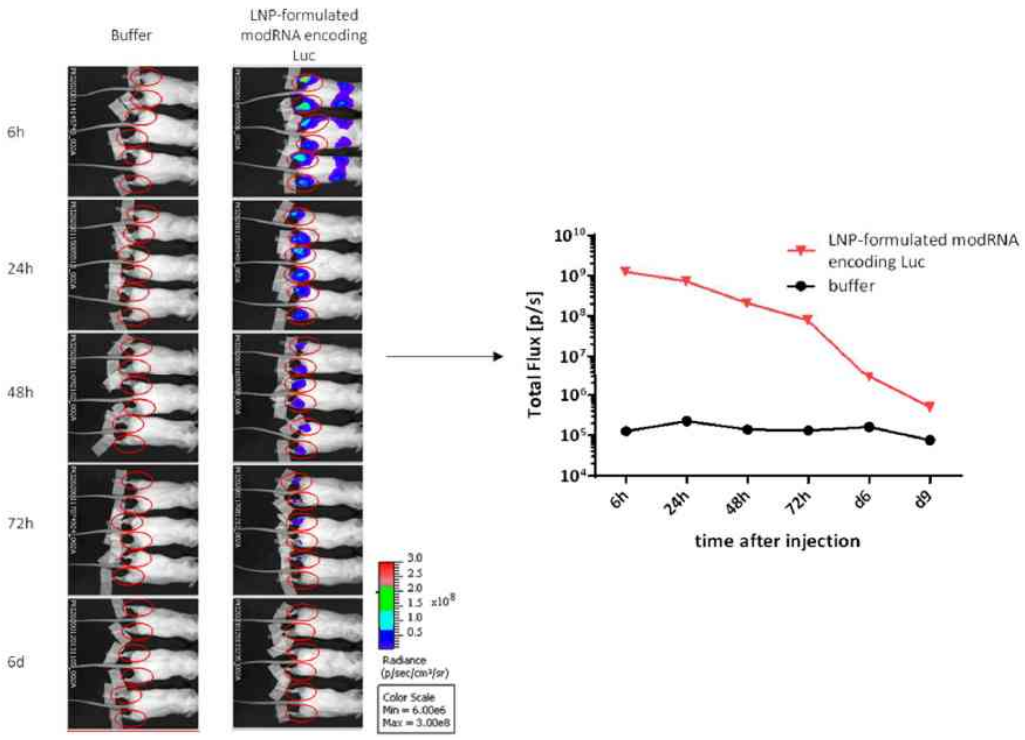

The distribution of a LNP with a comparable lipid composition to BNT162b2 but with a surrogate luciferase RNA (monitoring the ^{3}H-CHE lipid label), was investigated in blood, plasma and selected tissues in male and female Wistar Han rats over 48 hours after a single IM injection at 50 µg mRNA/animal (Study 185350; Tabulated Summary 2.6.5.5B). The greatest mean concentration of LNP was found remaining in the injection site at each time point in both sexes. Outside the injection site, low levels of radioactivity were detected in most tissues, with the greatest levels in plasma observed 1-4 hours post-dose. Over 48 hours, the LNP distributed mainly to liver, adrenal glands, spleen and ovaries, with maximum concentrations observed at 8-48 hours post-dose. Total recovery (% of injected dose) of LNP, for combined male and female animals, outside of the injection site was greatest in the liver (up to 18%) and was much less in the spleen (≤1.0%), adrenal glands (≤0.11%) and ovaries (≤0.095%). The mean concentrations and tissue distribution pattern were broadly similar between the sexes.

2.4.3.5. Metabolism

Of the four lipids used as excipients in the LNP formulation, two are naturally occurring (cholesterol and DSPC) and will be metabolized and excreted like their endogenous counterparts. The in vitro metabolic stability of the two novel lipids, ALC-0315 (aminolipid) and ALC-0159 (PEG-lipid), were evaluated in mouse, rat, monkey, and human liver microsomes, S9 fractions, and hepatocytes. ALC-0315 and ALC-0159 were stable (>82% remaining) over 120 min in liver microsomes and S9 fractions and over 240 min in hepatocytes in all species and test systems (Studies 01049-20008, 01049-20009, 01049-20010, 01049-20020, 01049-20021, and 01049-20022; Tabulated Summaries 2.6.5.10A and 2.6.5.10B).

Further study of the metabolism of ALC-0315 and ALC-0159 in vitro and in vivo evaluating the plasma, urine, feces, and liver from the rat PK study (Section 2.4.3.3.2) determined ALC-0315 and ALC-0159 are metabolized slowly (Study PF-07302048_05Aug20_043725; Tabulated Summaries 2.6.5.9, 2.6.5.10C, and 2.6.5.10D). ALC-0315 and ALC-0159 underwent hydrolytic metabolism of the ester and amide functionalities, respectively, and this hydrolytic metabolism was observed across the species evaluated (Figure 2.4.3-3 and Figure 2.4.3-4).

Figure 2.4.3-3. Proposed Biotransformation Pathway of ALC-0315 in Various Species

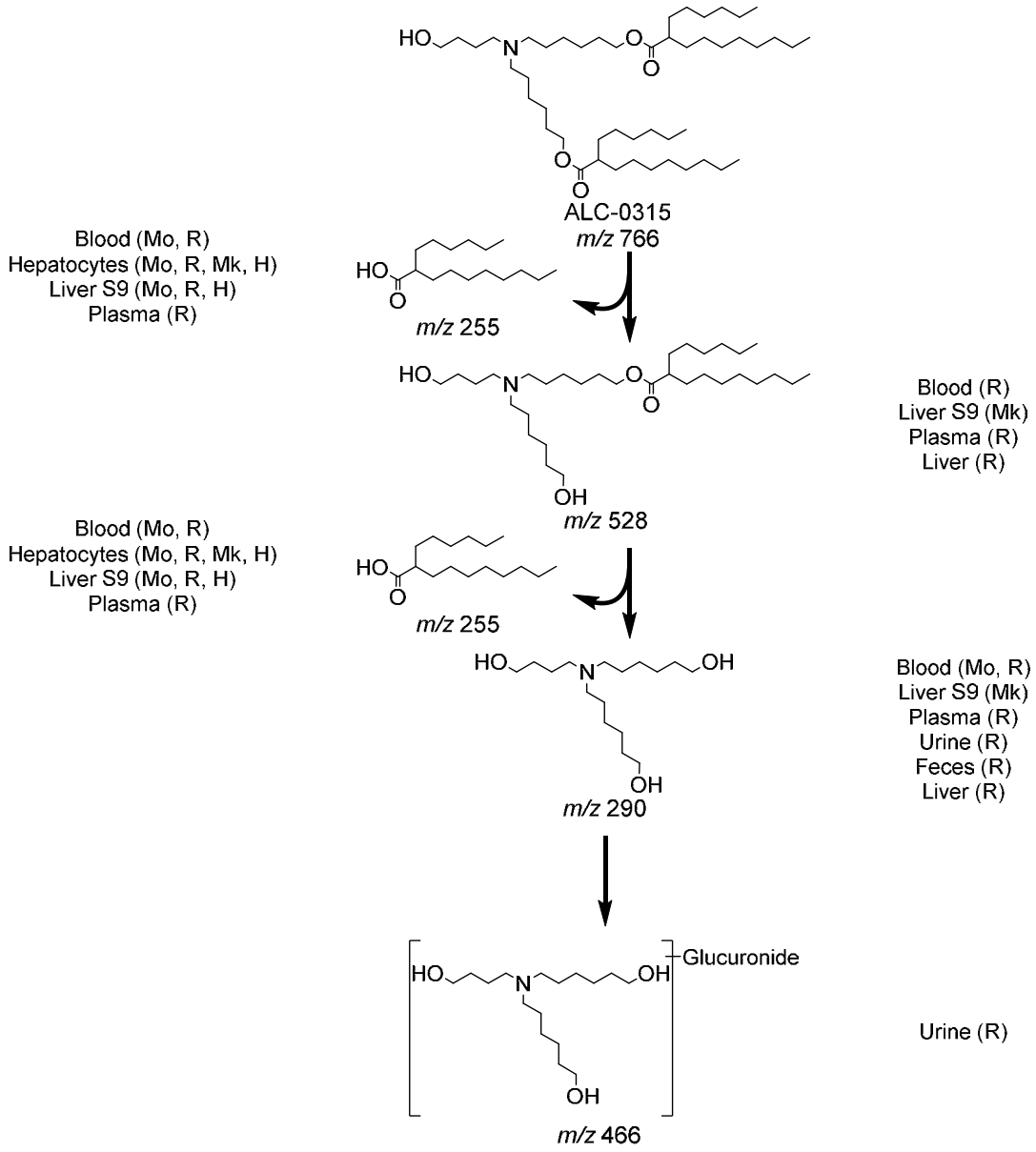

Metabolism of ALC-0315 occurs via two sequential ester hydrolysis reactions, first yielding the monoester metabolite (*m/z* 528) followed by the doubly deesterified metabolite (*m/z* 290). Subsequent metabolism of the doubly deesterified metabolite resulted in a glucuronide metabolite (*m/z* 466), which was only observed in urine from the rat PK study. Additionally, 6-hexyldecanoic acid (*m/z* 255), the acid product of both hydrolysis reactions of ALC-0315, was identified.

Figure 2.4.3-4. Proposed Biotransformation Pathway of ALC-0159 in Various Species

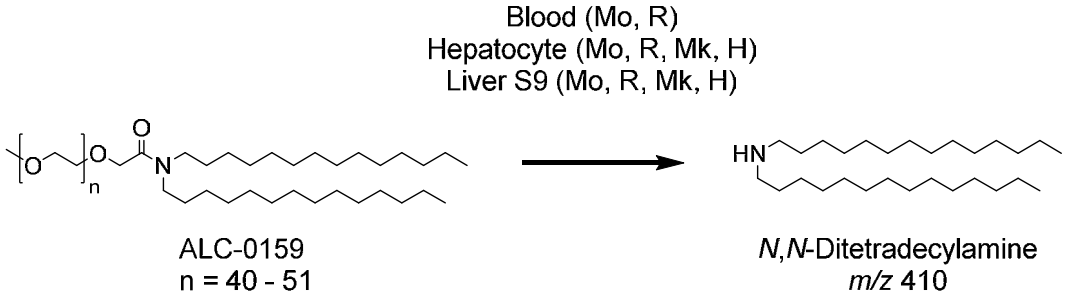

The primary route of metabolism identified for ALC-0159 involves amide bond hydrolysis yielding *N*,*N*-ditetradecylamine (*m/z* 410).

The protein encoded by the RNA in BNT162b2 is expected to be proteolytically degraded like other endogenous proteins. RNA is degraded by cellular RNases and subjected to nucleic acid metabolism. Nucleotide metabolism occurs continuously within the cell, with the nucleoside being degraded to waste products and excreted or recycled for nucleotide synthesis. Therefore, no RNA or protein metabolism or excretion studies will be conducted.

2.4.3.6. Excretion

In the rat PK study (Section 2.4.3.3.2), there was no detectable excretion of ALC-0315 and ALC-0159 in urine after IV administration of LNPs containing surrogate luciferase RNA at 1 mg/kg. The percent excreted unchanged in feces was ~1% for ALC-0315 and ~50% for ALC-0159. Metabolites of ALC-0315 were detected in the urine of rats (Figure 2.4.3-3). No excretion studies have been conducted with BNT162b2 for the reasons described in Section 2.4.3.5.

2.4.3.7. Pharmacokinetic Drug Interactions

No PK drug interaction studies have been conducted with BNT162b2.

2.4.4. TOXICOLOGY

2.4.4.1. Brief Summary

The nonclinical toxicity assessment of BNT162b2 (BioNTech code number BNT162, Pfizer code number PF-07302048) includes 2 GLP-compliant repeat-dose toxicity studies and a developmental and reproductive toxicity (DART) study in Wistar Han rats, outlined below in Table 2.4.4-1. The nonclinical safety evaluation included 2 variants of BNT162b2: V8 and V9. BNT162b2 (V9), the candidate submitted for licensure, differs from BNT162b2 (V8) only in the presence of optimized codons to improve antigen expression, but the amino acid sequences of the encoded antigens are identical. Two GLP repeat-dose toxicity studies for BNT162b2 (V8) and BNT162b2 (V9), one study for each variant, have been completed. In both studies, the nonclinical toxicology findings were similar between BNT162b2 (V9) and BNT162b2 (V8). BNT162b2 (V9) was assessed for development and reproductive toxicity in rats.

The IM route of exposure was selected as it is the intended route of clinical administration. The selection of rats as the toxicology test species is consistent with the WHO guidance documents on nonclinical evaluation of vaccines (WHO, 2005), which recommend that vaccine toxicity studies be conducted in a species in which an immune response is induced by the vaccine. Generation of an immune response to BNT162b2 has been confirmed in rats in both repeat-dose toxicity studies and the DART study. The Wistar Han rat is used routinely for regulatory toxicity studies, and there is an extensive historical safety database on this strain of rat.

Table 2.4.4-1. Overview of Toxicity Testing Program

Study[a]	Study (Sponsor) No.	Group/ Dose, µg RNA	Total Volume (µL)[b]	No. of Animals/ Group	Study Status
Repeat-Dose Toxicity					
17-Day, 2 or 3 Dose (1 Dose/Week) IM Toxicity With a 3 Week Recovery Phase in Rats[c,d]	38166	Control[e], 0	200[f]	15/sex	Completed
		BNT162b2 (V8)[i], 100	200[f]	15/sex	
17-Day, 3 Dose (1 Dose/Week) IM Toxicity With a 3 Week Recovery Phase in Rats[g]	20GR142	Saline[h], 0	60	15/sex	Completed
		BNT162b2 (V9)[i], 30	60	15/sex	
Developmental and Reproductive Toxicity					
Combined Fertility and Developmental Study (Including Teratogenicity and Postnatal Investigations) by the IM route in Rats[j]	20256434 (RN9391 R58)	Saline[h], 0	60	44 F	Completed
		BNT162b2 (V9)[i], 30	60	44 F	

a. All studies are GLP-compliant and were conducted in an OECD mutual acceptance of data-compliant member state.
b. Doses were administered as 1 application at 1 site unless otherwise indicated.
c. Study also evaluated the BNT162a1, BNT162b1, and BNT162c1 vaccine candidates.
d. QW x 3 (Days 1, 8, 15) for BNT162a1, BNT162b1, and BNT162b2 (V8); QW x 2 (Days 1, 8) for BNT162c1.
e. Phosphate buffered saline, 300 mM sucrose.
f. One application (100 µL) at 2 sites for a total dose volume of 200 µL.
g. Study also evaluated BNT162b3.
h. Sterile saline (0.9% NaCl).
i. BNT162b2 (V8) and BNT162b2 (V9) both encode the same amino acid sequence of the spike protein antigen with two prefusion conformation-stabilizing amino acids in the stalk.
j. Study also evaluated BNT162b1 and BNT162b3.

Administration of BNT162b2 by IM injection to male and female Wistar Han rats once every week for a total of 3 weekly cycles of dosing was tolerated without evidence of systemic toxicity in GLP-compliant repeat-dose toxicity studies. Expected inflammatory responses to the vaccine were evident such as edema and erythema at the injection sites, transient elevation in body temperature, elevations in WBCs and acute phase reactants, and lower A:G ratios. A transient elevation in GGT was noted in animals vaccinated with BNT162b2 (V8) in Study 38166 without evidence of microscopic changes in the biliary system or other hepatobiliary biomarkers but was not recapitulated in Study 20GR142. Injection site reactions were common in all vaccine-administered animals and were greater after boost immunizations. Changes secondary to inflammation included slight and transient reduction in body weights and transient reductions in RETIC, PLT, and RBC mass parameters. All changes in clinical pathology parameters and acute phase proteins were reversed at the end of

the recovery phase for BNT162b2 with the exception of higher RDW, higher globulins, and lower A:G ratios in animals administered BNT162b2 (V9). The higher RDW reflects prior RETIC increases. The higher A:G is due to low magnitude increases in globulins, which is an expected immune response to vaccine administration (Sellers et al, 2020).

Macroscopic pathology and organ weight changes were also consistent with immune activation and inflammatory response and included increased size of draining iliac lymph nodes and increased size and weight of spleen. Vaccine-related microscopic findings at the end of the dosing phase consisted of edema and inflammation in injection sites and surrounding tissues; increased cellularity in the draining (iliac) lymph nodes, bone marrow, and spleen; and hepatocyte vacuolation in the liver. Periportal vacuolation of hepatocytes was not associated with any microscopic evidence of hepatic injury or alterations in liver function tests and is interpreted to reflect hepatocyte uptake of the LNP lipids (Sedic et al, 2018). Microscopic findings at the end of the dosing phase were partially or completely recovered in all animals at the end of the recovery phase for BNT162b2. A robust immune response was elicited to the BNT162b2 antigen.

In the DART study, administration of BNT162b2 to female rats twice before the start of mating and twice during gestation at the human clinical dose (30 µg RNA/dosing day) was associated with nonadverse effects (body weight, food consumption, and localized effects in the injection site) after each dose administration. There were no effects of BNT162b2 administration on mating performance, fertility, or any ovarian or uterine parameters in the F0 female rats nor on embryo-fetal or postnatal survival, growth, or development in the F1 offspring through the end of lactation. A SARS-CoV-2 neutralizing antibody response to the vaccine was confirmed in F0 female rats prior to mating, at the end of gestation, and at the end of lactation and these neutralizing antibodies were also detectable in the F1 offspring (fetuses and pups).

2.4.4.2. Single-Dose Toxicity

A separate single-dose toxicity study with BNT162b2 has not been conducted.

2.4.4.3. Repeat-Dose Toxicity

2.4.4.3.1. Repeat-Dose Toxicity Study of Three LNP-Formulated RNA Platforms Encoding for Viral Proteins by Repeated Intramuscular Administration to Wistar Han Rats

The vaccine candidate BNT162b2 (V8), an LNP-formulated modified RNA vaccine expressing SARS-CoV-2 P2 S, was assessed in a GLP-compliant repeat-dose toxicity study in Wistar Han rats (Study 38166). This study also included assessment of 3 other LNP-formulated RNA vaccines, encoding either the SARS-CoV-2 P2 S or RBD antigens, which were not selected for licensure. For the purpose of this submission, only the study findings from the 100 µg BNT162b2 (V8) vaccine group are summarized; findings from the other vaccine candidates were generally similar.

Administration of BNT162b2 (V8) via IM injections once weekly for 3 administrations to male and female Wistar Han rats was tolerated without evidence of systemic toxicity. The

vaccine elicited a robust antigen-specific immune response and produced nonadverse macroscopic changes at the injection sites, spleen, and the draining lymph nodes; increased hematopoiesis in the bone marrow and spleen; periportal hepatocyte vacuolation; and clinical pathology changes consistent with an immune response. The findings in this study were fully recovered or showed evidence of ongoing recovery at the end of the 3-week recovery phase, and were consistent with those typically associated with the IM administration of LNP-encapsulated mRNA vaccines (Hassett et al, 2019).

Body weights were lower 24 hours after each BNT162b2 (V8) vaccine administration compared with predose values (down to 0.92x versus baseline) with evidence of weight gain (1.22x to 1.37x versus baseline) by the end of recovery. Body weight gain between the administrations was comparable to the buffer control group. There were no noteworthy effects on body weight at the end of the recovery phase. There were no effects on food consumption.

BNT162b2 (V8)-administered animals generally had higher body temperatures compared with buffer control animals at 4 and 24 hours postdose. Group mean temperatures in rats administered the BNT162b2 (V8) vaccine were higher, but within approximately 1°C of the group mean body temperature of buffer-administered animals. Individual rats administered BNT162b2 (V8) did not have body temperatures >40.0°C after administration.

Local reactions were observed in male and female animals dosed IM with BNT162b2 (V8). The incidence and severity of the reactions were higher after the second or third injections compared with the first injection. The majority of animals had very slight edema or rarely slight erythema after the first dose. After the second or third dose, the severity of edema and erythema increased up to moderate or rarely, severe grades. These observations resolved prior to the next injection or for recovery animals resolved during the 3-week recovery phase.

Most BNT162b2 (V8)-related changes in clinical pathology were consistent with an acute phase response and anticipated inflammation. Minor and variable alterations in other clinical pathology parameters were considered secondary effects of vaccination.

Expected immune responses to BNT162b2 (V8) were evident in hematology, such as elevations in mean neutrophil (up to 7.8x) eosinophil (up to 5.1x controls), basophil (1.47x controls), and LUC counts (up to 7.7x controls) and were highest on Day 17, 48 hours after the last injection. WBCs were higher (up to 2.2x controls) in the BNT162b2 (V8) vaccinated group on Day 17. PLT counts were slightly decreased on Day 17 (down to 0.66x controls). A transient reduction in RETIC counts (down to 0.28x controls) was only observed after the administration of the first dose on Day 4. Decreased RETICs were similarly observed in rats treated with the licensed LNP-siRNA pharmaceutical Onpattro™ (NDA # 210922) but have not been observed in humans treated with this biotherapeutic (Kozauer et al, 2018), suggesting this is a species-specific effect. A slight reduction in red blood cell mass (HGB down to 0.87x controls) was observed on Day 17. RETIC and RBC mass parameter decreases were likely secondary to the inflammation.

BNT162b2 (V8)-related changes in clinical chemistry included slightly higher GGT (a biomarker of biliary and not hepatocellular injury [Boone et al, 2005]) on Days 4 (up to 4.6x

controls) and 17 (up to 4.2x controls) without evidence of microscopic changes in the biliary system or other hepatobiliary biomarkers. Additionally, higher GGT was not observed in the second repeat-dose toxicity study (20GR142), conducted with the clinical candidate submitted for licensure. Albumin was slightly lower on Days 4 (down to 0.87x controls) and 17 (down to 0.89x controls) and globulin slightly higher on Day 17 (up to 1.2x controls). This resulted in the A:G ratio being slightly lower on Days 4 (down to 0.84x controls) and 17 (down to 0.76x controls). The effect on albumin and globulin were related to the vaccine-mediated inflammatory response as part of the negative and positive acute phase response, respectively (Sellers et al, 2020).

The acute phase proteins alpha-1-acid glycoprotein (up to 21x controls on Day 17) and alpha-2-macroglobulin (up to 217x controls on Day 17) were elevated in both males and females in the BNT162b2 (V8)-administered group on Days 4 and 17. Fibrinogen was higher in the vaccine-administered group (up to 3.1x controls), consistent with an acute phase response. Higher concentrations of acute phase proteins are an anticipated response to vaccination.

All changes in clinical pathology parameters and acute phase proteins were reversed at the end of the recovery phase.

Compared with the buffer control, there were no test-article related differences in the concentration of serum cytokines evaluated, in urinalysis parameters, or in ophthalmoscopic or auditory parameters.

BNT162b2 (V8)-related higher absolute and relative (to body) spleen weights (up to 1.62x controls) were evident and correlated with the macroscopic observation of increased spleen size and the increased hematopoiesis. This is likely secondary to immune responses induced by the BNT162b2 (V8) vaccine.

The most common macroscopic observation in the BNT162b2 (V8) group was a thickened injection site and/or induration noted for nearly all animals (16/20) at necropsy. This finding correlated with microscopic inflammation at the injection site. Macroscopic findings at the injection site were resolved at the end of the recovery phase. Enlarged spleen and iliac lymph nodes were noted in several animals in the BNT162b2 (V8)-administered group, which correlated microscopically to expansion of lymphoid and/or hematopoietic cells. The effects on the lymphoid organs are consistent with immune responses to the BNT162b2 (V8).

Vaccine-related microscopic findings at the end of dosing were evident in injection sites and surrounding tissues, in the draining (iliac) lymph nodes, bone marrow, spleen, and liver.

The inflammation at the injection site was characterized by infiltrates of macrophages, granulocytes, and lymphocytes into the muscle, and variably into the dermis and subcutis. Injection site inflammation was associated with moderate edema, mild myofiber degeneration, occasional muscle necrosis, and mild fibrosis. Injection site findings were consistent with an immune/inflammatory response to an IM vaccine administration.

In the draining (iliac) lymph node, increased cellularity of the follicular germinal centers and increased plasma cells (plasmacytosis) were variably present for all BNT162b2 (V8)-dosed animals. In addition, minimal to mild increases in the cellularity of bone marrow and

hematopoiesis in the spleen likely related to increased granulopoiesis and correlated with increased circulating neutrophils (which correlated with increased spleen size and weight) were present in BNT162b2 (V8)-dosed animals.

Vacuolation of hepatocytes (minimal to mild) in the portal regions of the liver were present for all BNT162b2 (V8)-dosed animals. The liver findings were not associated with changes in markers of hepatocyte injury (eg, AST or ALT). While GGT was elevated in vaccine-administered animals, it was not considered to be associated with the vacuolation of hepatocytes (Ennulat et al, 2010). The microscopic observation of liver vacuolation is believed to be associated with hepatocyte uptake of the LNP lipids (Section 2.4.3.4; Sedic et al, 2018).

Microscopic findings at the end of the dosing phase were partially or completely resolved in all animals at the end of the recovery phase. Inflammation at the injection site and surrounding tissues was less severe (minimal to mild) in animals administered BNT162b2 (V8) at the end of the 3-week recovery phase, indicating partial recovery. In the iliac lymph node, plasmacytosis was less severe, and macrophage infiltrates were present at the end of the 3-week recovery phase and reflect resolution of the inflammation noted at the end of the dosing phase.

All other observations in the bone marrow, spleen, and liver were fully resolved at the end of the 3-week recovery phase.

The immune response to the vaccine antigen was evaluated by S1-binding IgG and RBD-binding IgG ELISAs, and a SARS-CoV-2 S pseudotype neutralization (pVNT) assay on Days 17 and 38 (Section 2.4.2.1.4). The data demonstrate that BNT162b2 (V8) elicited a SARS-CoV-2 S-specific antibody response with high neutralizing activity.

In conclusion, administration of BNT162b2 (V8) by IM injection to male and female Wistar Han rats once every week for 3 doses, was tolerated at 100 µg RNA/dosing day without evidence of systemic toxicity.

2.4.4.3.2. 17-Day Intramuscular Toxicity Study of BNT162b2 (V9) in Wistar Han Rats with a 3-week Recovery

The vaccine candidate BNT162b2 (V9), an LNP-formulated modified RNA vaccine expressing SARS-CoV-2 P2 S, was assessed in a GLP-compliant repeat-dose toxicity study in Wistar Han rats (Study 20GR142). This study also included assessment of another LNP-formulated RNA vaccine candidate (BNT162b3) that will not be included in the licensure application. For the purpose of this submission, the study findings from the BNT162b2 (V9) vaccine are summarized; findings from the BNT162b3 vaccine candidate also tested in this study were generally similar. BNT162b2 (V9) was administered at 30 µg once weekly for 3 doses (Days 1, 8, and 15) followed by a 3-week recovery phase.

Administration of BNT162b2 (V9) via IM injections once weekly for 3 administrations to male and female Wistar Han rats was tolerated without evidence of systemic toxicity. The vaccine elicited a robust antigen-specific immune response and produced nonadverse macroscopic changes at the injection sites, spleen, and the draining lymph nodes; increased

hematopoiesis in the bone marrow and spleen; liver vacuolation; and clinical pathology changes consistent with an immune response. The findings in this study were either fully recovered or showed evidence of ongoing recovery at the end of the 3-week recovery phase, and were consistent with those typically associated with the IM administration of LNP-encapsulated mRNA vaccines (Hassett et al, 2019).

All animals administered BNT162b2 (V9) survived to scheduled necropsy. There were no test article-related clinical signs or body weight changes noted. Test article-related reduced mean food consumption was noted on Days 4 and 11 (down to 0.83x controls). Test article-related higher mean body temperature (maximum increase post each dose) compared with control animals was noted on Day 1 (up to 0.54°C), Day 8 (up to 0.98°C), and Day 15 (up to 1.03°C) postdose.

BNT162b2 (V9)-related injection site edema and erythema were noted on Days 1 (up to slight edema and very slight erythema), 8 (up to moderate edema and very slight erythema), and 15 (up to moderate edema and very slight erythema). The incidence and severity of the reactions were higher after the second or third injections compared with the first injection. Test article-related erythema and edema fully resolved prior to dose administration on Days 8 and 15. Injection site erythema and edema were fully resolved at the end of the recovery phase.

All clinical pathology changes (type and magnitude) were generally consistent with expected immune responses to the vaccine or secondary to inflammation.

There were higher WBCs (up to 2.95x controls), primarily involving neutrophils (up to 6.60x controls), monocytes (up to 3.30x controls), and LUC (up to 13.2x controls) and slightly higher eosinophils and basophils on Days 4 and 17. WBCs were higher on Day 17 as compared with Day 4. There were transiently lower RETICs on Day 4 (down to 0.27x controls) in both sexes and higher RETICs on Day 17 (up to 1.31x controls) in females only. Lower RBC mass parameters (down to 0.90x controls) were present on Days 4 and 17. All test article-related hematology and coagulation changes noted in the dosing phase were fully reversed after a 3-week recovery phase, with the exception of higher red cell distribution width (up to 1.21x controls) in animals administered BNT162b2 (V9). The higher RDW reflects prior reticulocyte increases.

There were lower A:G ratios (down to 0.82x) on Days 4 and 17. Higher fibrinogen levels were observed on Day 17 (up to 2.49x) when compared with control animals, consistent with an acute phase response. The acute phase proteins alpha-1-acid glycoprotein (up to 39x on Day 17) and alpha-2-macroglobulin (up to 71x on Day 17) were elevated in both males and females in the BNT162b2 (V9)-administered group on Days 4 and 17 with higher concentrations generally observed in males. All other changes in clinical pathology parameters were considered incidental. All test article-related clinical chemistry changes noted in the dosing phase were fully reversed after a 3-week recovery phase, except higher globulins (up to 1.08x controls) in animals administered BNT162b2 (V9) and lower A:G ratio (down to 0.91x controls) in females administered BNT162b2 (V9), reflecting vaccine-related immune response.

Test article-related higher group mean absolute and relative spleen weights (compared to body weight) were noted in males that had received BNT162b2 (V9) (up to 1.42x) and females (up to 1.59x) relative to control group means. There were no other test article-related changes in organ weights. At the end of the recovery phase, spleen weights were within normal limits.

Test article-related macroscopic findings included the observation of enlarged draining lymph nodes (2/20 animals) and pale/dark (5/20 animals) or firm (6/20 animals) injection sites in animals administered BNT162b2 (V9). These changes fully recovered, except for partial recovery of enlarged draining nodes, suggesting recovery in progress.

Test article-related microscopic pathology findings were observed at the injection site and in the draining (iliac) and inguinal lymph nodes, spleen, bone marrow, and liver for both vaccine candidates. All microscopic findings were nonadverse, as there was no evidence of systemic toxicity or clinical signs of illness or lameness.

At the end of the dosing phase, test article-related mixed cell inflammation (mild to moderate) and edema (mild to moderate) at the injection site were consistent with findings typically associated with the IM administration of LNP-encapsulated mRNA vaccines (Hassett et al, 2019). These findings correlated with macroscopic observations of abnormal color (dark/pale) and consistency (firm). At the end of the 3-week recovery phase, there was full recovery for injection site edema and partial recovery for injection site inflammation, suggesting recovery in progress.

At the end of the dosing phase, test article-related findings in the draining (iliac) and inguinal lymph nodes (up to moderately increased cellularity of plasma cells and germinal centers), spleen (minimally increased cellularity of hematopoietic cells and germinal centers), and the bone marrow (minimal increased cellularity of hematopoietic cells) were present. These changes are secondary to immune activation and/or inflammation at the injection site. The presence of plasma cells (interpreted as plasmablasts) in the draining (iliac) and inguinal lymph nodes is consistent with a robust immunological response to the vaccines. These observations correlated with macroscopic observations of abnormal size (enlarged) in the lymph nodes and spleen and increased spleen weights. At the end of the 3-week recovery phase, full recovery of increased cellularity of hematopoietic cells in the spleen and bone marrow, with partial recovery (recovery in progress) of increased cellularity of plasma cells and germinal centers in the draining and inguinal lymph nodes, and increased cellularity of the germinal centers in the spleen.

At the end of the dosing phase, the test article-related microscopic finding of minimal peri-portal hepatocyte vacuolation was not associated with hepatocellular damage or alterations in liver function tests. The liver vacuolation is believed to be associated with hepatocyte uptake of the LNP lipids (Section 2.4.3.4; Sedic et al, 2018). At the end of 3-week recovery phase, this finding was completely recovered.

Administration of 3 once weekly doses of BNT162b2 (V9) elicited SARS-CoV-2 neutralizing antibody responses in males and females at the end of the dosing (Day 17) and recovery phases (Day 21) of the study. SARS-CoV-2 neutralizing antibody responses were

not observed in animals prior to vaccine administration or in saline-administered control animals.

In conclusion, administration of BNT162b2 (V9) at 30 µg RNA/dosing day via IM injections weekly for 3 administrations to male and female Wistar Han rats was tolerated without evidence of systemic toxicity. Dosing of BNT162b2 (V9) produced changes consistent with an inflammatory response and immune activation. The findings in this study are consistent with those typically associated with the IM administration of LNP-encapsulated mRNA vaccines.

2.4.4.4. Genotoxicity

No genotoxicity studies are planned for BNT162b2 as the components of the vaccine construct are lipids and RNA and are not expected to have genotoxic potential (WHO, 2005).

2.4.4.5. Carcinogenicity

Carcinogenicity studies with BNT162b2 have not been conducted as the components of the vaccine construct are lipids and RNA and are not expected to have carcinogenic or tumorigenic potential. Carcinogenicity testing is generally not considered necessary to support the development and licensure of vaccine products for infectious diseases (WHO, 2005).

2.4.4.6. Reproductive and Developmental Toxicity

Reproductive and developmental toxicity assessments were made with BNT162b2 (V9) (Study 20256434). BNT162b2 was administered by IM injection at the human clinical dose (30 µg RNA/dosing day) to 44 female Wistar Han rats (F0) 21 and 14 days prior to mating with untreated males and on GD 9 and 20, for a total of 4 dosing days. A separate control group of 44 F0 females received saline by the same route and regimen.

Following completion of a mating phase with untreated males, 22 rats/group underwent caesarean-section on GD 21 and were submitted to routine embryo-fetal development evaluations. The remaining 22 rats/group were allowed to litter and development of the offspring was observed until PND 21.

There were no BNT162b2-related deaths during the study. IM administration of BNT162b2 before and during gestation to female Wistar rats resulted in nonadverse clinical signs and macroscopic findings localized to the injection site as well as transient, nonadverse body weight and food consumption effects after each dose administration. These maternal findings are all consistent with administration of a vaccine and an inflammatory/immune response.

There were no BNT162b2-related effects on any mating or fertility parameters. There were no BNT162b2-related effects on any ovarian, uterine, or litter parameters, including embryo-fetal survival, growth, or external, visceral, or skeletal malformations, anomalies, or variations. There were no effects of BNT162b2 administration on postnatal offspring (F1) development, including postnatal growth, physical development (pinna unfolding and eye

opening), reflex ontogeny (pre-weaning auditory and visual function tests), macroscopic observations, and survival.

All F0 females administered BNT162b2 developed SARS-CoV-2 neutralizing antibodies and these antibodies were also detectable in all fetuses and pups from the caesarean and littering groups, respectively. The animals in the saline control group did not exhibit an immune response to BNT162b2.

In conclusion, administration of BNT162b2 to female rats twice before the start of mating and twice during gestation at the human clinical dose was associated with nonadverse effects (body weight, food consumption, and effects localized to the injection site) after each dose administration. However, there were no effects of BNT162b2 administration on mating performance, fertility, or any ovarian or uterine parameters in the F0 female rats nor on embryo-fetal or postnatal survival, growth, or development in the F1 offspring. An immune response was confirmed in F0 female rats following administration of each vaccine candidate and these responses were also detectable in the F1 offspring (fetuses and pups).

Macroscopic and microscopic evaluation of male and female reproductive tissues from the repeat-dose toxicity studies with BNT162b2 showed no evidence of toxicity.

2.4.4.7. Local Tolerance

Local tolerance of IM administration of BNT162b2 was evaluated by injection site observations and macroscopic and microscopic examination of injection sites in the repeat-dose toxicity studies and is described in Section 2.4.4.3.

2.4.4.8. Other Toxicity Studies

2.4.4.8.1. Phototoxicity

Phototoxicity studies with BNT162b2 have not been conducted.

2.4.4.8.2. Antigenicity

Immunogenicity was evaluated as part of the primary pharmacodynamic studies (Section 2.4.2.1). Serology data from the repeat-dose toxicity studies shows a robust antigen-specific immune response to BNT162b2.

2.4.4.8.3. Immunotoxicity

Stand-alone immunotoxicity studies with BNT162b2 have not been conducted. However, immunotoxicological endpoints were collected as part of the repeat-dose toxicity studies; there were no adverse effects observed and no significant effects on measured cytokines.

2.4.4.8.4. Mechanistic Studies

Mechanistic studies with BNT162b2 have not been conducted.

2.4.4.8.5. Dependence

Dependence studies with BNT162b2 have not been conducted.

2.4.4.8.6. Studies on Metabolites

Stand-alone studies with administration of metabolites of BNT162b2 have not been conducted.

2.4.4.8.7. Studies on Impurities

Stand-alone studies with administration of impurities of BNT162b2 have not been conducted.

2.4.4.8.8. Other Studies

No other studies with BNT162b2 evaluated in this submission have been conducted.

2.4.4.9. Target Organ Toxicity

Based on data from the GLP repeat-dose toxicity studies (Section 2.4.4.3), administration of BNT162b2 was well tolerated without any evidence of systemic toxicity. BNT162b2 administration was associated with local reactogenicity at the injection site and expected inflammatory responses, including increases in lymphoid cells in draining lymph nodes and spleen. Microscopic findings within injection sites, which were partially reversed by the end of recovery, support this conclusion. The liver finding was reversible, not associated with changes in markers of hepatocyte injury and not considered adverse. The elevated levels of GGT in Study 38166 were not recapitulated in Study 20GR142 and were not associated with hepatobiliary changes microscopically. Elevated GGT was not attributed to the hepatocyte vacuolation (Ennulat et al, 2010).

2.4.5. INTEGRATED OVERVIEW AND CONCLUSIONS

The nonclinical program demonstrates that BNT162b2 is immunogenic in mice, rats, and nonhuman primates, and the toxicity studies support the licensure of this vaccine. Preclinical assessments in mice and nonhuman primates demonstrate that BNT162b2 elicits a rapid antibody response with measurable SARS-CoV-2 neutralizing titers after a single dose and substantial increases in titers after a second dose that exceed titers in sera from SARS-CoV-2/COVID-19-recovered patients. A Th1-dominant T cell response was evident in both mice and nonhuman primates. In a SARS-CoV-2 rhesus challenge model, BNT162b2 provided complete protection in the lungs, as determined by lack of detectable viral RNA, and there was no evidence of vaccine-elicited disease enhancement.

An IV rat PK study, using an LNP with the identical lipid composition as BNT162b2, demonstrated that the novel lipid excipients in the LNP formulation, ALC-0315 and ALC-0159, distribute from the plasma to the liver. While there was no detectable excretion of either lipid in the urine, the percent of dose excreted unchanged in feces was ~1% for ALC-0315 and ~50% for ALC-0159. Further studies indicated metabolism played a role in the elimination of ALC-0315. Biodistribution was assessed using luciferase expression as a surrogate reporter formulated like BNT162b2, with the identical lipid composition. After IM injection of the LNP-formulated RNA encoding luciferase in BALB/c mice, luciferase protein expression was demonstrated at the site of injection 6 hours post dose and was not detected after 9 days. Luciferase was detected to a lesser extent in the liver; expression was present at 6 hours after injection and was not detected by 48 hours after injection. After IM administration of a radiolabeled LNP-mRNA formulation containing ALC-0315 and ALC-0159 to rats, the percent of administered dose was also greatest at the injection site. Outside of the injection site, total recovery of radioactivity was greatest in the liver and much lower in the spleen, with very little recovery in the adrenal glands and ovaries. The metabolism of ALC-0315 and ALC-0159 was evaluated in blood, liver microsomes, S9 fractions, and hepatocytes from mice, rats, monkeys, and humans. The in vivo metabolism was examined in rat plasma, urine, feces, and liver samples from the PK study. Metabolism of ALC-0315 and ALC-0159 appears to occur slowly in vitro and in vivo. ALC-0315 and ALC-0159 are metabolized by hydrolytic metabolism of the ester and amide functionalities, respectively, and this hydrolytic metabolism is observed across the species evaluated.

Administration of BNT162b2 by IM injection to male and female Wistar Han rats once every week for a total of 3 weekly cycles of dosing was tolerated without evidence of systemic toxicity in GLP-compliant repeat-dose toxicity studies. Expected immune responses to the vaccine were evident such as edema and erythema at the injection sites, transient elevation in body temperature, elevations in WBCs and acute phase reactants, and decreased A:G ratios. Injection site reactions were common in all vaccine-administered animals and were greater after boost immunizations. Changes secondary to inflammation included slight and transient reductions in body weights and transient reductions in RETIC, PLT, and RBC mass parameters. All changes in hematology parameters and acute phase proteins were similar to control at the end of the recovery phase for BNT162b2 with the exception of higher RDW and lower A:G ratios in animals administered BNT162b2 (V9). Macroscopic pathology and organ weight changes were also consistent with immune activation and inflammatory response and included increased size of draining iliac lymph nodes and increased size and

weight of spleen. Vaccine-related microscopic findings at the end of dosing for BNT162b2 were evident in injection sites and surrounding tissues, in the draining iliac lymph nodes, bone marrow, spleen, and liver. Microscopic findings at the end of the dosing phase were partially (recovery in progress) or completely recovered in all animals at the end of the recovery phase for BNT162b2. A robust immune response was elicited to the BNT162b2 vaccine antigen.

Administration of BNT162b2 to female rats twice before the start of mating and twice during gestation at the human clinical dose (30 µg RNA/dosing day) was associated with nonadverse effects (body weight, food consumption and effects localized to the injection site) after each dose administration. There were no effects of BNT162b2 administration on mating performance, fertility, or any ovarian or uterine parameters in the F0 female rats nor on embryo-fetal or postnatal survival, growth, or development in the F1 offspring. An immune response was confirmed in F0 female rats following administration of BNT162b2 and this response was also detectable in the F1 offspring (fetuses and pups).

In summary, the nonclinical package summarized above supports the BLA of BNT162b2 administered twice by IM injection at a dose of 30 µg RNA.

2.4.6. LIST OF LITERATURE REFERENCES

Barry MA, May S, Weaver EA. Imaging luciferase-expressing viruses. Methods Mol Biol 2012;797:79-87.

Boone L, Meyer D, Cusick P, et al. Selection and interpretation of clinical pathology indicators of hepatic injury in preclinical studies. Vet Clin Pathol 2005;34(3):182-8.

Cai Y, Zhang J, Xiao T, et al. Distinct conformational states of SARS-CoV-2 spike protein. Science 2020:10.1126/science.abd4251.

Chen C-Y, Tran DM, Cavedon A, et al. Treatment of Hemophilia A Using Factor VIII Messenger RNA Lipid Nanoparticles. Mol Ther Nucleic Acids 2020;20:534-44.

Elia U, Ramishetti S, Dammes N, et al. Design of SARS-CoV-2 RBD mRNA Vaccine Using Novel Ionizable Lipids. bioRxiv 2020.10.15.341537.

Ennulat D, Magid-Slav M, Rehm S, et al. Diagnostic performance of traditional hepatobiliary biomarkers of drug-induced liver injury in the rat. Toxicol Sci 2010;116(2):397-412.

Fukuchi M, Saito R, Maki S, et al. Visualization of activity-regulated BDNF expression in the living mouse brain using non-invasive near-infrared bioluminescence imaging. Mol Brain 2020;13(1):122.

Hassett KJ, Benenato KE, Jacquinet E et al. Optimization of lipid nanoparticles for intramuscular administration of mRNA vaccines. Molecular Therapy Nucleic Acids 2019;15:1-11.

Jeon YH, Choi Y, Kang JH, et al. In vivo monitoring of DNA vaccine gene expression using firefly luciferase as a naked DNA. Vaccine 2006;24(16):3057-62.

Jiang S, Hyllyer C, Du L. Neutralizing antibodies against SARS-CoV-2 and other human coronaviruses. Science and society. Trends Immunol 2020;41(5)(May):355-9.

Ke Z, Oton J, Qu K, et al. Structures, conformations and distributions of SARS-CoV-2 spike protein trimers on intact virions. Nature 2020;10.1038/s41586-020-2665-2.

Kim JY, Ko JH, Kim Y, et al. Viral load kinetics of SARS-CoV-2 infection in first two patients in Korea. J Korean Med Sci 2020;35(7)(Feb):e86.

Kozauer NA, Dunn WH, Unger EF, et al. CBER multi-discipline review of Onpattro. NDA 210922. 10 Aug 2018. Available at: https://www.accessdata.fda.gov/drugsatfda_docs/nda/2018/210922Orig1s000MultiR.pdf. 02 Aug 2020.

Munster VJ, Feldmann F, Williamson BN, et al. Respiratory disease in rhesus macaques inoculated with SARS-CoV-2. Nature 2020 (May). Available from: https://doi.org/10.1101/2020.03.21.001628. Accessed: 24 Sep 2020.

Pallesen J, Wang N, Corbett KS, et al. Immunogenicity and structures of a rationally designed prefusion MERS-CoV spike antigen. Proc Natl Acad Sci USA 2017;114(35):E7348-57.

Pardi N, Hogan MJ, Pelc RS, et al. Zika virus protection by a single low-dose nucleoside-modified mRNA vaccination. Nature 2017;543(7644):248-51.

Pardi N, Parkhouse K, Kirkpatrick E, et al. Nucleoside-modified mRNA immunization elicits influenza virus hemagglutinin stalk-specific antibodies. Nat Comm 2018;9(1)(08):3361.

Sahin U, Karikó K, Türeci Ö. mRNA-based therapeutics - developing a new class of drugs. Nat Rev Drug Discov 2014;13(10):759-80.

Sedic M, Senn J, Lynn A, et al. Safety Evaluation of Lipid Nanoparticle–Formulated Modified mRNA in the Sprague- Dawley Rat and Cynomolgus Monkey. Vet Path 2018;55(2):341-54.

Sellers RS, Nelson K, Bennet B, et al. Scientific and regulatory policy committee points to consider*: approaches to the conduct and interpretation of vaccine safety studies for clinical and anatomic pathologists. Toxicol Pathol 2020;48(2):257-76.

Singh DK, Ganatra SR, Singh B, et al. SARS-CoV-2 infection leads to acute infection with dynamic cellular and inflammatory flux in the lung that varies across nonhuman primate species. bioRxiv 2020:06.05.136481. Accessed: 24 Sep 2020.

Truong B, Allegri G, Liu X-B, et al. Lipid nanoparticle-targeted mRNA therapy as a treatment for the inherited metabolic liver disorder arginase deficiency. Proc Natl Acad Sci USA 2019;116(42):21150-9.

US Department of Health and Human Services, Food and Drug Administration, Center for Biologics Evaluation and Research. Development and licensure of vaccines to prevent COVID-19. In: Guidance for industry. Rockville, MD: Food and Drug Administration; 2020: 21 pages.

World Health Organization. WHO guidelines on nonclinical evaluation of vaccines. Annex 1. In: World Health Organization. WHO technical report series, no. 927. Geneva, Switzerland; World Health Organization; 2005:31-63.

World Health Organization. Annex 2. Guidelines on the nonclinical evaluation of vaccine adjuvants and adjuvanted vaccines. In: WHO technical report series no. 987. Geneva, Switzerland: World Health Organization; 2014: p. 59-100.

Wrapp D, Wang N, Corbett KS, et al. Cryo-EM structure of the 2019-nCoV spike in the prefusion conformation. Science 2020;367(6483):1260-3.

Yong CY, Ong HK, Yeap SK, et al. Recent advances in the vaccine development against middle east respiratory syndrome-coronavirus. Front Microbiol 2019;10:1781.

Zakhartchouk AN, Sharon C, Satkunarajah M, et al. Immunogenicity of a receptor-binding domain of SARS coronavirus spike protein in mice: implications for a subunit vaccine. Vaccine 2007;25(1):136-43.

Zhou M, Zhang X, Qu J. Coronavirus disease 2019 (COVID-19): a clinical update. Front Med 2020(Apr):1-10.

Zost S, Gilchuk P, Chen R, et al. Rapid isolation and profiling of a diverse panel of human monoclonal antibodies targeting the SARS-CoV-2 spike protein. BioRxiv posted May13, 2020, www.biorxiv.org/content/10.1101/2020.05.12.091462v1.

Zou L, Ruan F, Huang M, et al. SARS-CoV-2 viral load in upper respiratory specimens of infected patients. N Engl J Med 2020;382(12)(03):1177-9.